SOILS AND FOUNDATIONS Vol. 25, No. 3, 1-18, Sept. 1985
Japanese Society of Soil Mechanics and Foundation Engineering

UNDRAINED SHEAR CHARACTERISTICS OF NORMALLY CONSOLIDATED PEAT UNDER TRIAXIAL COMPRESSION AND EXTENSION CONDITIONS

HAREYUKI YAMAGUCHI*, YOSHINORI OHIRA**, KEIJI KOGURE** and SHIGERU MORI***

ABSTRACT

Both vertical and horizontal samples of undisturbed fibrous peat, which were obtained by maintaining the axes of thin-walled tubes parallel to the vertical and horizontal directions in peat ground, were used in this investigation. These samples contained organic matter in the amount of 10%-80%. After normal isotropical consolidation of the samples in the triaxial cell, undrained compression and extension tests with pore water pressure measurement were performed, and the influences of confining pressure, loading path, amount of organic matter and fabric anisotropy on the undrained shear behavior of peat were investigated. Test results indicate that the undrained shear behavior of saturated peat can be discussed based on the principle of effective stress, in the same manner as inorganic soils. However, as the anisotropic fabric of fibrous peat which had formed during accumulation still remained after the isotropic consolidation, anisotropic shear behavior was observed ; the undrained deformation-strength properties observed in the compression test were considerably distinct from those obtained in the extension test. Moreover, it was also found that the normally consolidated fibrous peat had a cohesion intercept due to the effect of tension in the fibers, and undrained-strength parameters were found to be greater than those of inorganic soils.

Furthermore, based on the test results, the authors proposed a new method of predicting stress-strain behavior of peat under triaxial compression and extension conditions.

Key words : angle of internal friction, anisotropy, cohesion, consolidated undrained shear, highly organic soil, shear strength, stress path, triaxial compression test (**IGC** : D 6/D 5)

INTRODUCTION

It has been said that peat which is mainly composed of fibrous organic matters, i. e. partly decomposed plants such as leaves and stems, shows unique mechanical properties in

* Associate Professor, Department of Civil Engineering, The National Defense Academy, Yokosuka, Kanagawa.
** Professor, Department of Civil Engineering, The National Defense Academy, Yokosuka, Kanagawa.
*** Graduate Student, Department of Civil Engineering, The National Defense Academy, Yokosuka, Kanagawa.

Manuscript was received for review on December 9, 1983.
Written discussions on this paper should be submitted before April 1, 1986, to the Japanese Society of Soil Mechanics and Foundation Engineering, Sugayama Bldg. 4 F, Kanda Awaji-cho 2-23, Chiyoda-ku, Tokyo 101, Japan. Upon request the closing date may be extended one month.

comparison with those of inorganic soils such as clay and sandy soils. Also, it is generally said that it is material which strongly shows strength anisotropy. However, there have been only a few systematic investigations concerning the mechanical properties of highly organic soils and peats ; in particular, there have been very few studies on the shear characteristics of peat. Therefore, there are many points which must be solved regarding the fundamental shear characteristics of peat. The explanation of such problems will be useful for practical geotechnical problems such as slope stability or bearing capacity of peat ground.

In this paper, based on the results obtained from undrained triaxial compression and extension tests——which were performed by using both the vertical and horizontal samples of undisturbed peat——the influences of confining pressure, loading path, amount of organic matter and fabric anisotropy on the undrained shear characteristics of normally consolidated peat are presented. Moreover, based on the experimental facts and the original Cambridge theory, the authors also proposed a new method to explain systematically the stress-strain behavior of peat under triaxial compression and extension conditions.

EXPERIMENTS

Peat Tested

The sample used in this investigation is fibrous peat with the physical properties shown in Table 1. The saturated undisturbed sample was brought from a riverside near Ohmiya city, Saitama Prefecture. The sample contained a considerable amount of vegetal fibers, and we could therefore not determine

Table 1. Physical properties of peat

Properties		Amounts
Natural water content	$w_n(\%)$	110~1200
Natural void ratio	e_n	5~19
Specific gravity	G_p	1.52~2.56
Degree of saturation	$S_r(\%)$	100
Ignition loss	$L_{ig}(\%)$	10~85
Degree of decomposition	$D(\%)$	25~65
Potential of hydrogen	pH	5~7
Liquid limit	LL(%)	—
Plastic limit	PL(%)	—

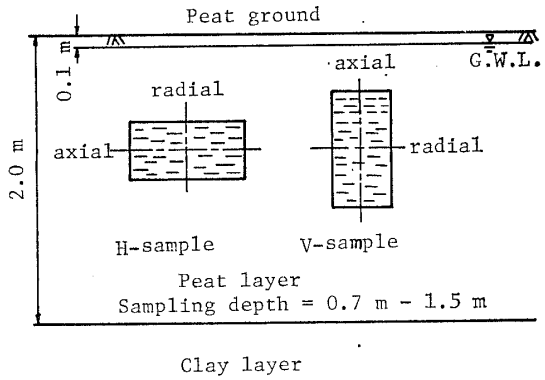

Fig. 1. *V* and *H* samples from peat ground

the values of the liquid and plastic limits of sample. The amount of organic matter is indicated by the ignition loss, denoted by the symbol L_{ig}. It is defined as the ratio of the mass lost by heating at a temperature of 800 °C to the total dry mass of the peat sample. As illustrated in Fig. 1, the ground water level (G. W. L.) of the peat ground was only slightly below the ground surface, and the peat layer under the ground surface reached a depth of about 2 m. The samples were obtained by using thin-walled tubes 75 mm in diameter and 500 mm in length. In order to ensure the least variation among the individual samples, they were sampled from a depth range of 0.7 m to 1.5 m below the ground surface in the same vicinity. In sampling, care was taken to maintain the axes of the samples parallel to the vertical and horizontal directions in the peat ground, and these samples were designated as vertical (*V*) and horizontal (*H*) samples. The total unit weight of each peat sample was about 10.8 kN/m^3 and the sample was normally consolidated under the present maximum effective overburden pressure of about 10 kPa. The samples were waxed and wrapped in the field, and then stored in a water bath at the laboratory.

The undisturbed sample was gently removed from the thin-walled tube. As shown in Photo. 1, a specimen, 50 mm in diameter and 125 mm in length, was trimmed from the sample with a very fine wire saw and a cutter, and was then placed on a saturated porous stone which was mounted on

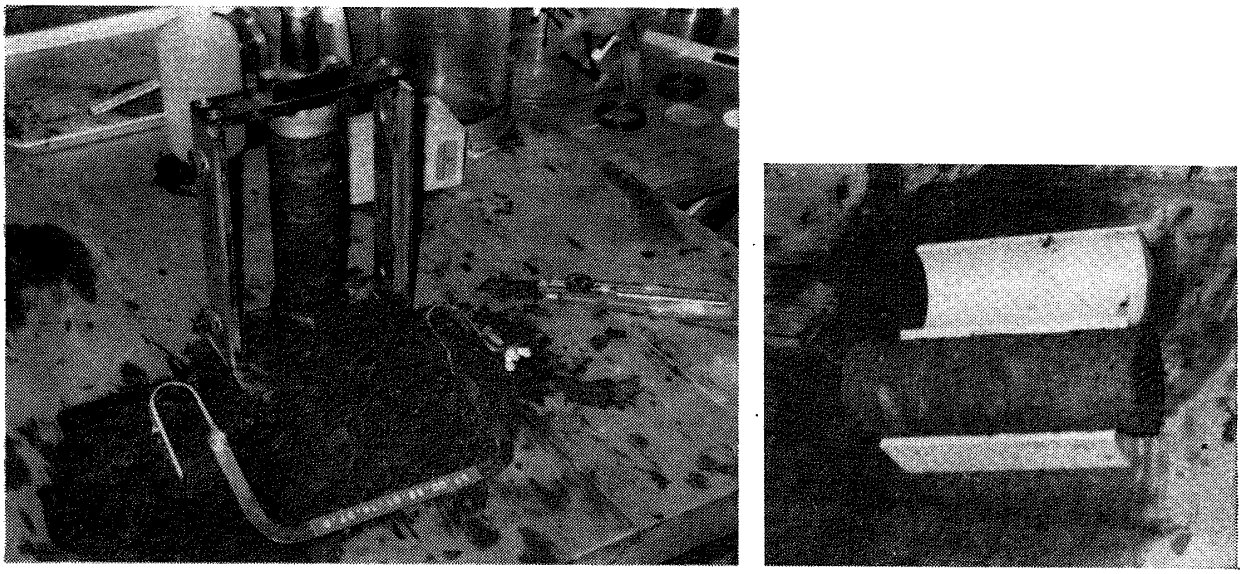

Photo. 1. Peat sample tested

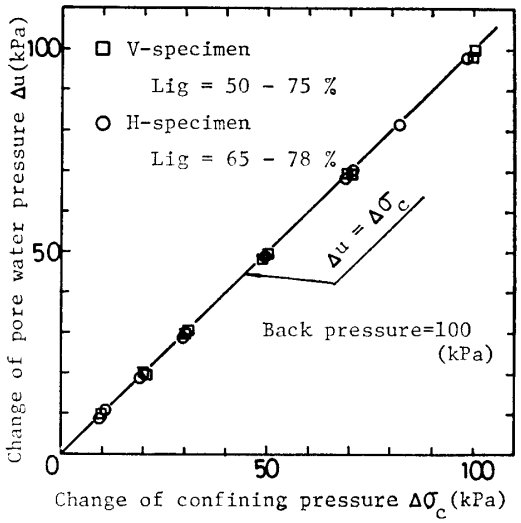

Fig. 2. Changes of pore water pressure due to changes of confining pressure under undrained conditions

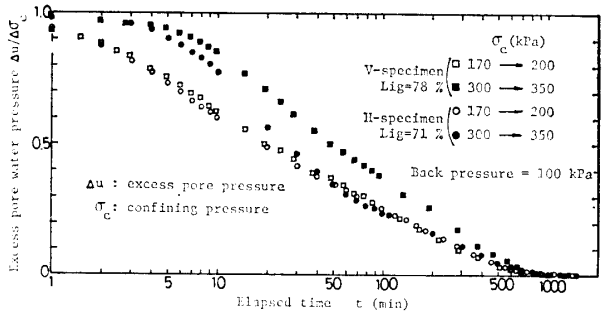

Fig. 3. Excess pore water pressure vs. elapsed time curves during isotropic consolidation

the base of a triaxial cell. A slotted filter paper drain was wrapped around the specimen in order to accelerate drainage. All specimens were isotropically normally consolidated in the triaxial cell and then sheared under undrained conditions.

Testing Procedure

In the consolidation process, an initial back pressure of 100 kPa was applied to all specimens to insure saturation, and an all-round pressure in the range of 10 kPa-50 kPa was raised in several steps to its final value. The completion of primary consolidation was specified by the dissipation of excess pore water pressure Δu at the final-stage pressure-increase increment, and the pore pressure parameter, value of B, was checked at each stage (see Fig. 2). The loading duration of the all-round pressure in each stage was specified to be one day ; the duration after reaching the final cell pressure, however, was specified to be two days. Therefore, the excess pore water pressure prior to shear was essentially equal to zero. Typical excess pore water pressure vs. time curves during consolidation of V and H specimens are shown in Fig. 3. The time required for dissipation of excess pore water pressure was found to be from 700 min to 1000 min. After the completion of consolidation, as shown in Table 2, six

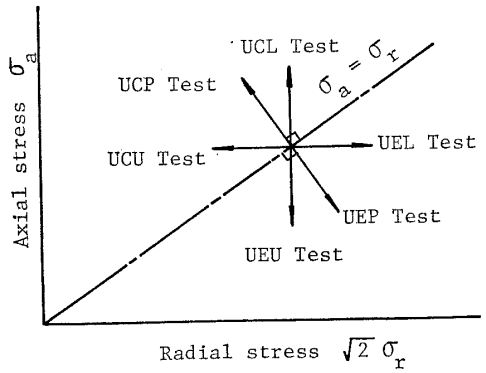

Fig. 4. Various loading paths under undrained conditions

series of undrained shear tests on the specimens, with consolidation pressure σ_c' ranging from about 100 kPa to 350 kPa, were performed under the following conditions :

i) UCL Test : Radial stress σ_r constant, axial stress σ_a increased ; i. e. loading compression test.

ii) UCP Test : Radial stress decreased and axial stress increased so that the total mean principal stress $p=(\sigma_a+2\sigma_r)/3$ remained constant ; i. e. constant total p compression test.

iii) UCU Test : Radial stress decreased, axial stress constant ; i. e. unloading compression test.

iv) UEL Test : Radial stress increased, axial stress constant ; i. e. loading extension test.

v) UEP Test : Radial stress increased and axial stress decreased so that the total mean principal stress remained constant ; i. e. constant total p extension test.

vi) UEU Test : Radial stress constant, axial stress decreased ; i. e. unloading extension test.

The total stress paths corresponding to the loading conditions mentioned above are illustrated in a Rendulic diagram (see Fig. 4). In addition, the UCL Test was also carried out under another condition only on the *H*-specimens ; that is, as shown in Table 3 (test results at failure are also shown in this table), after the end of consolidation at the consolidation pressure σ_c' of about 100 kPa, the drainage line was closed and the confining pressure σ_c of 200 kPa was raised to 300 kPa or 400 kPa, and then the shear test was carried out.

In Table 2, the tests in group (A) were performed under the strain-controlled condition with the rate of axial strain of 0.05%/min, and those in group (B) were performed under the stress-controlled condition. The

Table 2. Types of tests

	No.	Test type	Specimen	w_n(%)	G_p	L_{ig}(%)	σ_c'(kPa)	w_c(%)
(A)	V-29	UCL	*V*-specimen	1095	1.582	83	100	421
	V-28	〃	〃	118	2.56	10	147	63
	V-30	〃	〃	481	1.997	40	199	158
	V-20	〃	〃	942	1.552	78	100	417
	V-4	〃	〃	860	1.721	70	197	266
	V-9	〃	〃	852	1.687	71	343	205
	H-3	〃	*H*-specimen	923	1.747	73	99	380
	H-5	〃	〃	997	1.690	73	197	294
	H-7	〃	〃	774	1.763	59	299	211
	H-14	UEU	〃	830	1.726	71	96	364
	H-16	〃	〃	1000	1.552	74	98	413
	H-15	〃	〃	926	1.710	70	199	282
(B)	H-2	UCL	*H*-specimen	941	1.623	78	97	414
	H-6	UCP	〃	1114	1.603	79	98	446
	H-4	UCU	〃	924	1.782	67	98	389
	H-9	UEP	〃	899	1.742	68	99	349
	H-12	UEL	〃	895	1.705	72	96	387
	H-8	UEP	〃	1027	1.725	65	149	338
	H-19	UEU	〃	885	1.712	72	98	376

(A) : Strain control (rate of axial strain $\dot{\varepsilon}_a$=0.05%/min), (B) : Stress control, w_n : Natural water content, G_p : Specific gravity, L_{ig} : Ignition loss, σ_c' : Preshear consolidation pressure, w_c : Preshear water content.

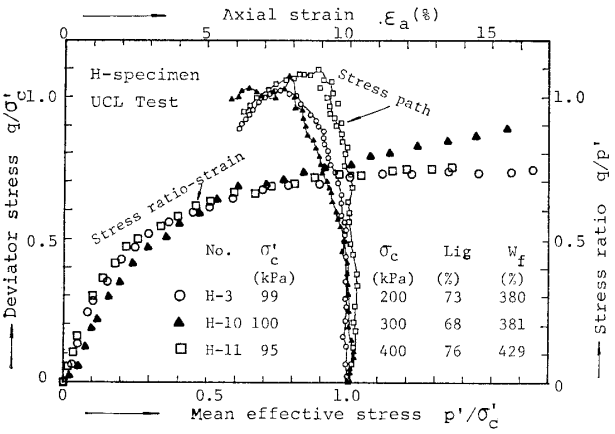

Fig 5. Influence of magnitude of confining pressure prior to shear on undrained shear behavior

Table 3. Stress conditions prior to shear and at failure in UCL Test

No.	End of isotropic consolidation		Beginning of shear		Failure $(\sigma_{af}-\sigma_{rf})_{max}$			
	σ_c (kPa)	σ_c' (kPa)	σ_c (kPa)	σ_c' (kPa)	σ_{af} (kPa)	σ_{rf} (kPa)	σ_{af}' (kPa)	σ_{rf}' (kPa)
H-3	200	99	200	99	302	200	144	42
H-10	201	100	300	101	408	300	151	43
H-11	199	95	400	98	505	400	149	44

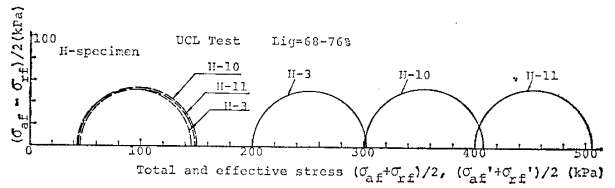

Fig. 6. Mohr circles in UCL Test with different magnitudes of confining pressures

pore water pressure was measured at the bottom of the specimen.

EXPERIMENTAL RESULTS

Influence of Confining Pressure

The normalized effective stress paths and stress ratio vs. axial strain curves are shown in Fig. 5, where $q=\sigma_a-\sigma_r$, $p'=(\sigma_a'+2\sigma_r')/3$ and ε_a is the axial strain and σ_c' is the effective stress at the beginning of shear. As shown in Table 3, these results were obtained from the UCL Test on the *H*-specimens with three different confining pressures σ_c. The effective stress σ_c' at the end of consolidation was almost equal to that at the beginning of shear. This suggests that the increment of confining pressure corresponds to that of pore water pressure. Then, as is obvious from Fig. 5, in spite of the different magnitudes of confining pressures, the effective stress paths during undrained shear almost coincide and to a great extent the same loci of stress-strain curves are observed. It is further seen from Fig. 6 that the angle of shear resistance ϕ_u given from the three Mohr circles in terms of total stress is almost equal to zero, and their effective Mohr circles, which are shown with the dotted circles, agree well. Hanrahan (1954) also reported similar results from the unconsolidated undrained test on saturated peat. Accordingly, the undrained shear behavior of fibrous peat, as well as of saturated inorganic soils, is not significantly affected by the confining pressure, and can be discussed in the conventional way based on the concept of effective stress.

Influence of Loading Path

The normalized stress-strain curves and effective stress paths obtained from the tests of group (B) in Table 2 are plotted in Figs. 7 and 8, respectively. The consolidation pressure σ_c' was about 100 kPa for all specimens except for specimen *H*-8, for which the pressure was about 150 kPa. It can be seen from these two figures that the undrained compression or extension behavior during the three different loading conditions

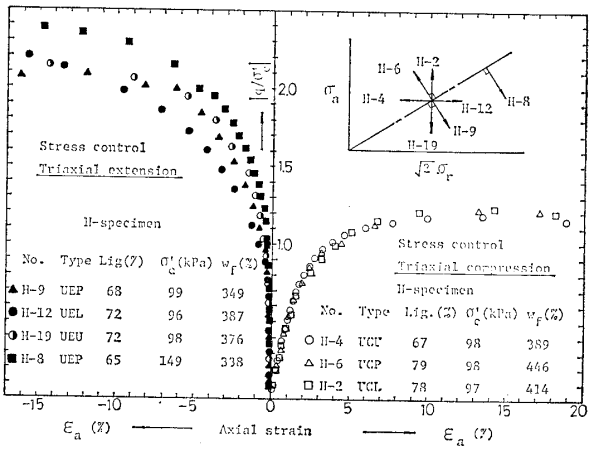

Fig. 7. Deviator stress vs. axial strain curves for various loading conditions

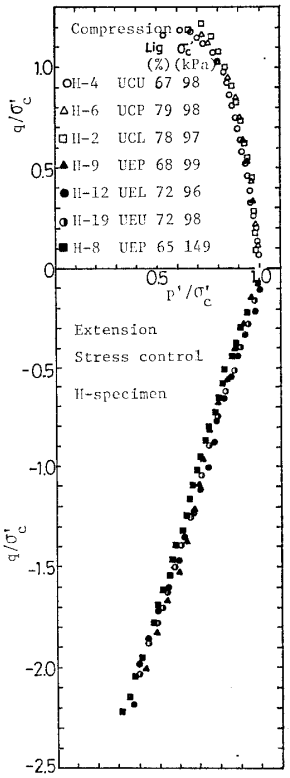

Fig. 8. Normalized effective stress paths for various loading conditions

is for the most part essentially independent of the total stress path to failure ; if normally consolidated specimens are subjected to these various types of undrained tests in compression or extension stress space, the effective stress path and the undrained strength normalized by consolidation pressure σ_c' will become the same for each type of loading. That is, as a first approximation, it can be said that the undrained shear behavior in the same stress space (compression or extension) for fibrous peat as well as for inorganic clay soils is dependent only upon the initial conditions existing before shear and is independent of the way in which the shear is applied.

However, as shown in Figs. 7 and 8, the difference between compression and extension shear behavior is very remarkable. The stress-strain curves in the extension tests on the *H*-specimens show a rapid increase in deviator stress for the changes in axial strain at small values of axial strain. Also, the *H*-specimens show a very large effective angle of shearing resistance and undrained shear strength in the extension tests. Such a tendency is probably due to the anisotropic fabric of fibrous peat.

Influence of Amount of Organic Matter

Based on the results of the UCL Test on

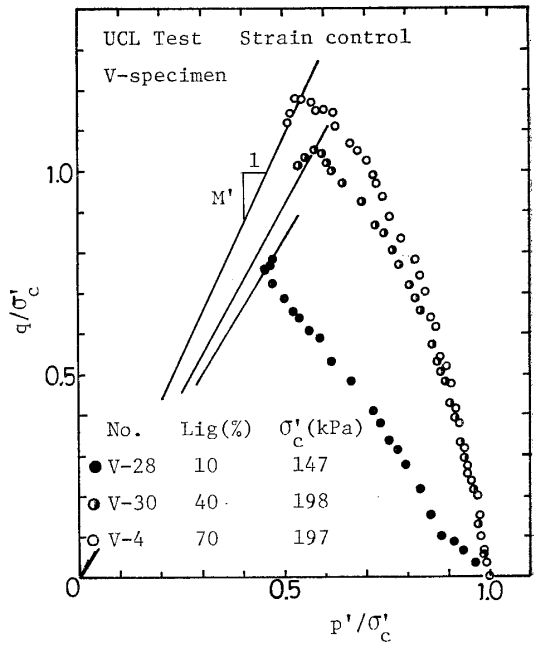

Fig. 9(a). Influence of amount of organic matter on effective stress path (*V*-specimens)

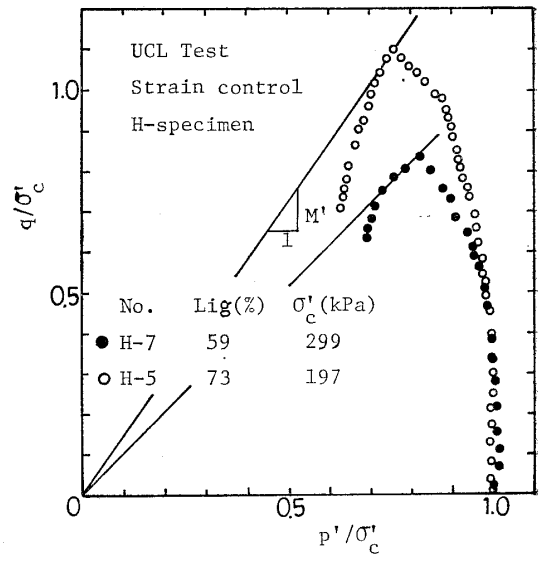

Fig. 9(b). Influence of amount of organic matter on effective stress path (*H*-specimens)

the V-specimens (V-4, V-28 and V-30) and the H-specimens (H-5 and H-7), the influence of the amount of organic matter on undrained compression behavior was investigated. The normalized effective stress paths are shown in Figs. 9(a) and (b). As can be seen in these figures, the effective stress paths of peat are influenced considerably by the amount of organic matter and move away from the origin with an increase in this amount. In particular, in the V-specimen results, such a tendency appears to a marked extent in the range of organic matter content between 10% and 40%. For both V and H specimens which contain an organic matter content of about 70%, the effective stress paths indicate that the deviator stress q increases to the maximum value under almost constant effective mean stress p' during undrained shear. Adams (1965) also observed a similar stress-path locus from an undrained triaxial compression test on saturated fibrous peat with an L_{ig} of 77%-80%. It is also seen from Fig. 9 that the values of maximum deviator stress and shear stress ratio mobilized at failure (represented by the symbol M') increase with the increase in the amount of organic matter. This M' corresponds to the effective angle of shearing resistance. From the results of undrained and drained triaxial compression tests on reconstituted samples of mixed clay and peat (Muck) in various ratios of mass, Tsushima et al (1982) showed that the value of the angle of shearing resistance increased with the increase in the amount of peat, and that the value of the dilatancy coefficient also increased in proportion to the amount of peat. That is, it can probably be said that the shear behavior of soil is considerably influenced by the amount of vegetal matter, and that large strength-parameter values may be obtained with an increase in the amount of vegetal matter involved.

Fig. 10 shows the normalized pore water pressure $\Delta u/\sigma_c'$ vs. ε_a curves for V and H specimens in the UCL Test. The amount of organic matter has a significant influence on pore water pressure behavior for specimens containing a relatively low organic matter

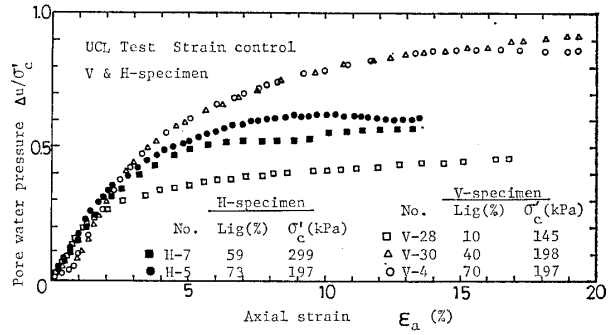

Fig. 10. Influence of amount of organic matter on pore water pressure vs. axial strain curves

content of 40% or less. The values of $\Delta u/\sigma_c'$ for the V-specimen V-28, with an L_{ig} of 10%, are very small in comparison with those for the V specimens V-30 (L_{ig}=40%) and V-4 (L_{ig}=70%) at strains larger than 3%. In the cases of V and H specimens with organic matter content greater than 40%, the $\Delta u/\sigma_c'$ vs. ε_a curves almost agree, and there is no apparent influence related to the amount of

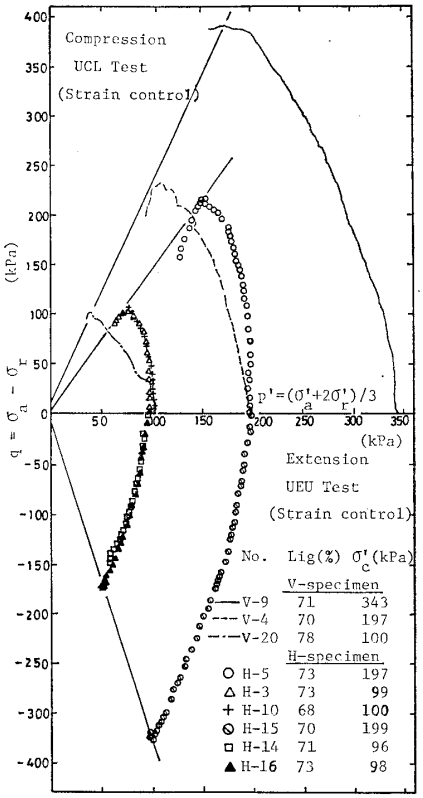

Fig. 11. Effective stress paths under compression and extension conditions

vegetal matter.

Behavior under Compression and Extension Conditions

The results of the strain-controlled UCL Test on *V*-specimens and the UCL and UEU Tests on *H*-specimens are plotted in Figs. 11–13. The specimens of peat used in these tests, containing almost the same amount of organic matter (about 70%), were isotropically normally consolidated in the range of consolidation pressure σ_c' between approximately 100 kPa and 350 kPa. As shown in Figs. 11–13, the undrained shear behavior of the specimens in the compression test is very different from that of the *H*-specimens in the same test. Similarly, for the same *H*-specimens, the behavior under compression conditions is quite distinct from that under extension conditions. As pointed out in Figs. 7 and 8, this suggests that the anisotropic fabric of fibrous peat still remains after isotropic consolidation, and this characteristic is particularly apparent during shear. From the difference between the effective stress paths for *V* and *H* specimens under compression, it can be said that the developing pore water pressure due to the deviator stress component for *V*-specimens at any identical shear stress ratio is large compared with that for *H*-specimens. Namely, the *V*-specimen under compression takes the form of a fabric enriched with a negative dilatancy.

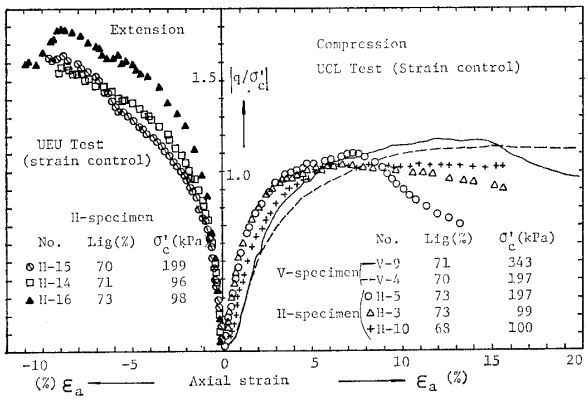

Fig. 12. Deviator stress vs. axial strain curves under compression and extension conditions

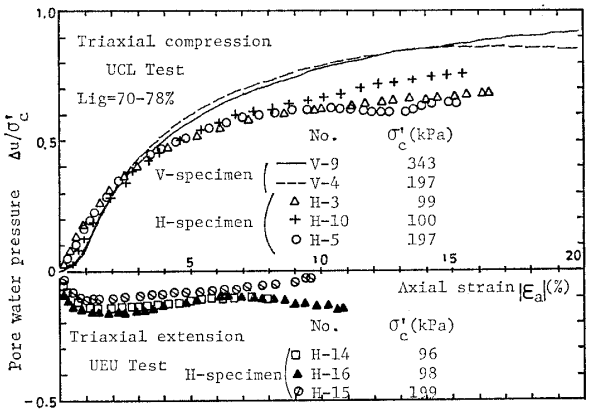

Fig. 13. Pore water pressure vs. axial strain curves under compression and extension conditions

It is also expected from Fig. 11 that normally consolidated peat not only has a large effective angle of shearing resistance but also shows a vertical intercept due to the development of tension in the fibers extending across the failure plane. The shear stress ratio at failure in the compression test on *V*-specimens and in the extension test on *H*-specimens will become very large compared with that in the compression test on *H*-specimens. It is for this reason that the orientation in fibers for *V*-specimens during compression shear may be very similar to that for *H*-specimens during extension shear.

From the results of normalized q/σ_c' vs. ε_a in Fig. 12 and $\Delta u/\sigma_c'$ vs. ε_a in Fig. 13, it is seen that the undrained shear behavior under compression or extension conditions can be approximately normalized by the effective stress σ_c' at the beginning of shear. Similar results can be read from Figs. 7 and 8. However, rapid changes in deviator stresses at small strains are observed in the extension test on *H*-specimens. As can be seen in Fig. 13, this is probably due to the development of negative pore water pressure, which produces an increase in effective stress during extension shear.

Undrained Strength Parameters

Based on the test data on normally consolidated *V* and *H* specimens with an L_{ig} of about 70% described in the previous section, only the stress states at failure, which are

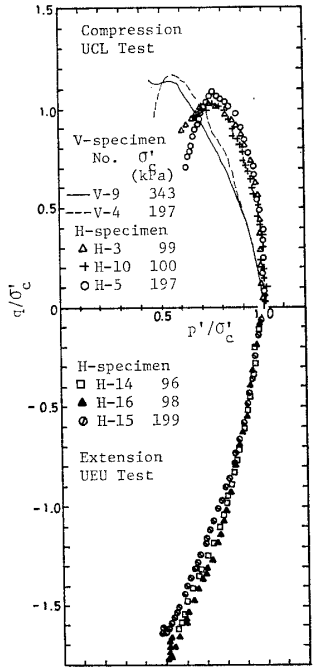

Fig. 14. Normalized effective stress paths in UCL and UEU Tests

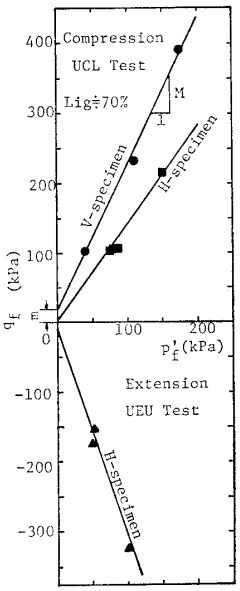

Fig. 15. States of stress at failure plotted in q vs. p' plane

determined from deviator stress maximum criteria, are plotted again Figs. 15 and 16, where q_f and p_f' are equal to q and p' at failure, and c_u is the undrained shear strength $|q_f/2|$. Also, the symbols M and m in Fig. 15 are, respectively, the inclination and vertical intercept of the q_f vs. p_f' relationship, approximated by a straight line.

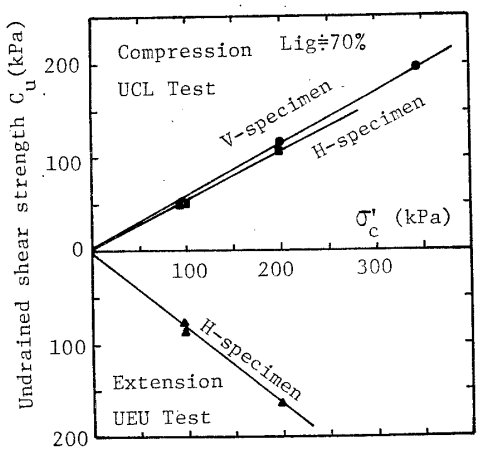

Fig. 16. c_u vs. σ_c' relationships for normally consolidated peat

In the UCL and UEU Tests, the effective angle of shearing resistance ϕ', the cohesion intercept c', and the pore water pressure parameter at failure A_f are given by the following equations :

UCL Test (Loading compression) :

$$\left.\begin{aligned} &\phi'=\sin^{-1}\left(\frac{3M}{6+M}\right),\quad c'=\frac{3-\sin\phi'}{6\cos\phi'}m,\\ &A_f=\frac{\Delta u_f}{\Delta\sigma_{af}} \end{aligned}\right\} \quad (1)$$

UEU Test (Unloading extension) :

$$\left.\begin{aligned} &\phi'=\sin^{-1}\left(\frac{3|M|}{6-|M|}\right),\quad c'=\frac{3+\sin\phi'}{6\cos\phi'}|m|,\\ &A_f=1-\frac{\Delta u_f}{\Delta\sigma_{af}} \end{aligned}\right\} \quad (2)$$

where Δu_f and $\Delta\sigma_{af}$ are the change in pore water pressure and the axial stress to failure. Since normally consolidated peat has a vertical intercept on the q_f vs. p_f' plane of Fig. 15, the c_u vs. σ_c' relationships in Fig. 16 also have vertical intercepts, but can be represented approximately by straight lines. The inclinations $\overline{c_u/\sigma_c'}$ of these straight lines correspond to the rate of increase in undrained shear strength due to consolidation. In addition to these values of ϕ', c' and A_f calculated by Eqs. (1) and (2), $\overline{c_u/\sigma_c'}$ in Fig. 16 and the values of axial strain at failure ε_f are summarized in Table 4. The value of ϕ' for soils must be within the range of 0°–90°. Then, from Eqs. (1) and (2), the range of

Table 4. Strength parameters of normally consolidated peat

	V-specimen	*H*-specimen	
	compression	compression	extension
M	2.14	1.43	−2.97
m (kPa)	7	1	−5
ϕ' (°)	52	35	—
c' (kPa)	4	0.5	—
$\overline{c_u/\sigma_c'}$	0.55	0.53	0.80
A_f	0.71∼0.93	0.54∼0.56	0.94∼0.97
ε_f (%)	12∼15	6∼8	8∼9

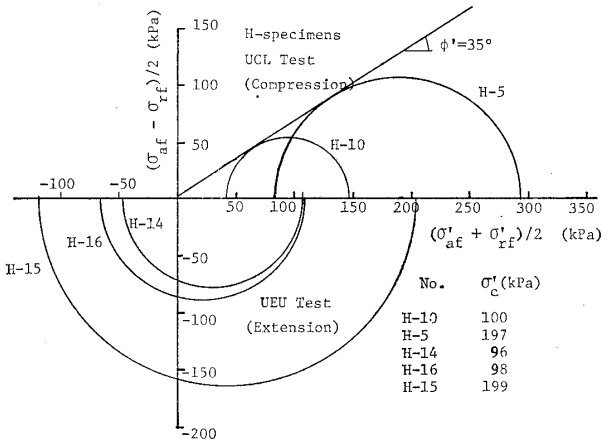

Fig. 17. Effective Mohr circles in UCL and UEU Tests on *H*-specimens

M values corresponding to the condition $0°<\phi'<90°$ is given as follows :

$$-1.5<M<3 \qquad (3)$$

That is, if the value of M obtained from the tests satisfies Eq. (3), by using the values of M and m from Eqs. (1) and (2), it will be possible to calculate the values of ϕ' and c'. However, as can be seen in Table 4, the value of M obtained from the UEU Test on *H*-specimens was −2.97. So, for the *H*-specimens, we could not determine the values of ϕ' and c' under the extension condition. Fig. 17 shows the effective Mohr circles obtained from the UCL and UEU Tests on *H*-specimens. In the UEU Test, the magnitude of pore water pressure at failure becomes larger than the axialstress σ_a. That is, the negative value in effective axial stress σ_{af}' is measured at failure, and as the value of consolidation pressure σ_c' increases, this σ_{af}' shows further increased negative value. Therefore, it was impossible to determine the two values of ϕ' and c' for *H*-specimens under the extension condition. As the most probable explanation for the results obtained, it may be said that the tension in vegetal fibers contributes to the strength parameters of peat to a greater extent than might be expected, and the effect of tension depends on the magnitude of consolidation pressure. Hanrahan (1954) reported from the results of unconsolidated undrained tests on saturated fibrous peats that the developing excess pore water pressure at failure became larger than the magnitude of confining pressure ; he reported also that negative lateral effective stress was obtained. Thus, in the case of the extension test on *H*-specimens in this experiment, it may be said that such a tendency is produced by the considerable development of tension in fibers extending across the failure plane.

As seen in Table 4, the fibrous peat shows predominantly anisotropic strength properties. The ϕ' of 52° from the compression test on *V*-specimens was very large compared with the ϕ' of 35° for *H*-specimens. Also, the values of $\overline{c_u/\sigma_c'}$ larger than 0.5 were measured, and the value of 0.8 from the extension test on *H*-specimens was a particularly large value. Such large values in the strength parameters of peat have been also reported by other research workers. Table 5 shows the results of typical triaxial compression carried out by other researchers on undisturbed and remoulded peats, where the ICU Test corresponds to the UCL Test in this paper, where the K_0CU Test corresponds to the UCL Test on K_0 consolidated samples, and where the ICD and K_0CD Tests are standard drained triaxial tests on samples consolidated under isotropic stress and K_0 conditions. Values of ϕ' larger than 50° have been measured by other research workers. The very large value of $\phi'=78.3°$ was indicated by Oikawa et al (1980). Also, Adams (1962), Ozden et al (1970) and Oikawa et al (1980) indicated that normally consolidated fibrous peats had a cohesion intercept c'. The value of c' for undisturbed Muskeg, ac-

Table 5. Strength parameters of normally consolidated peat according to various research reports

Authors	Samples	w_n(%)	G_p	L_{ig}(%)	c'(kPa)	ϕ' or ϕ_d(°)	c_u/σ_c'	Tests
Adams (1962)	Muskeg (U)	375~430	1.62~1.70	77.5~87.5	14	50 51		ICU ICD
Adams (1965)	Muskeg (U)	200~600	1.62~1.73		0	48		ICU
Ozden et al (1970)	Muskeg (U)	800	1.57	96	5	46		ICU
Tsushima et at (1977)	Muck (R)		1.84~1.86	57~58	0 0 0 0	51.9 60.2 51.5 51.5	0.54 0.52	ICU KoCU ICD KoCD
Oikawa et al (1980)	Muck (U)		1.62~1.77	56.1~67.4	1.0	78.3	0.63	ICU
Tsushima et al (1982)	Muck (R)		1.82	56	0	51.1 50.2		ICU ICD
Edil et al (1981)	Peat (U) Peat (U) Peat (U)	240 600 510	1.94 1.92 1.41	20* 31* 64*	0 0 0	50.2 53.8 57.4		KoCU KoCU KoCU

*: Fiber content, (U): Undisturbed sample, (R): Remolded sample

cording to Adams (1962), was 14 kPa. The values of c_u/σ_c' for Ohmiya peat were very near the values for Muck obtained by Tsushima et al (1977) and Oikawa et al (1980). The values of A_f in the UCL Test on V-specimens and in the UEU Test on H-specimens were closer to unity. However, this value from the UCL Test on H-specimens was about 57% in the UEU Test, and the value of ε_f=6%-8% for H-specimens in the UCL Test was very small compared with that of ε_f=12%-15% for V-specimens in the same test.

UNDRAINED STRESS-STRAIN RELATIONSHIP FOR NORMALLY CONSOLIDATED PEAT

Assumptions

The stress-strain equations of peat under triaxial compression and extension conditions derived by the present authors are based on the theory of Roscoe et al (1963) and the methods of Mitachi et al (1979) and Yamaguchi et al (1983) which make use of the dilatancy function, which represents approximately the experimental dilatancy vs. stress ratio relationships of clay soils. The assumptions of the present authors, then, are essentially the same as those of these three research groups. Further, in this paper, based on the experimental facts, we made the following assumptions in order to derive the stress-strain equations for normally consolidated peat :

(i) The total change of void ratio during shear d_e is represented by the sum of the change due to the increment of effective mean stress $(d_e)_c$ and that due to the increment of deviatoric stress $(d_e)_d$:

$$d_e=(d_e)_c+(d_e)_d \qquad (4)$$

As shown in Fig. 8, from the volume change behavior in isotropic compression-swelling tests on V-specimens of peat, by using the inclinations λ^*, κ^* of the straight lines plot-

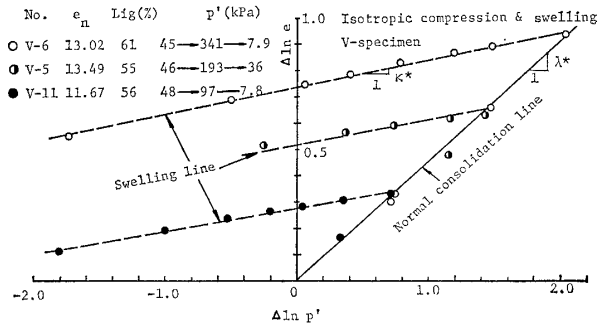

Fig. 18. Changes of void ratio during isotropic compression and swelling

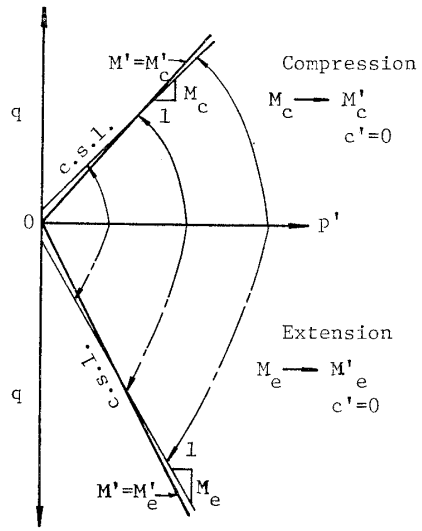

Fig. 19. Schematic diagram of stress states at critical state

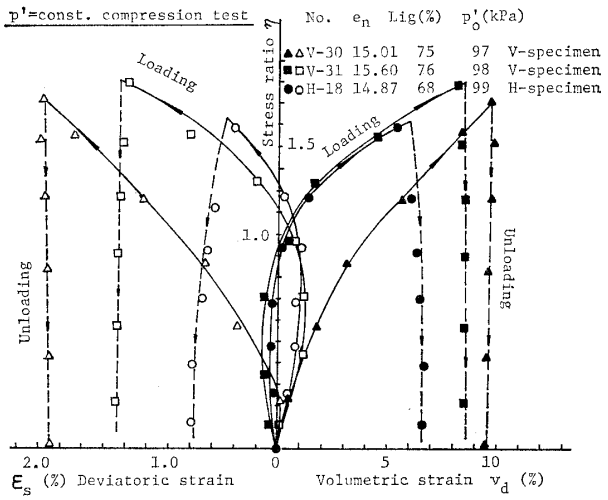

Fig. 20. Loading-unloading behavior of peat (*V* and *H* specimens) under constant mean effective principal stress

ted in the $\Delta\ln e$ vs. $\Delta\ln p'$ plane, the $(d_e)_c$ in the above equation and its elastic and plastic components $(d_e)_c^e$, $(d_e)_c^p$ are approximately expressed as follows :

$$(d_e)_c=-\lambda^* e_0\left(\frac{p'}{p_0'}\right)^{-\lambda^*}\frac{dp'}{p'} \quad (5)$$

$$(d_e)_c^e=e_0\left[(\lambda^*-\kappa^*)\left(\frac{p'}{p_0'}\right)^{-(\lambda^*-\kappa^*)}-\lambda^*\times\left(\frac{p'}{p_0'}\right)^{-\lambda^*}\right]\frac{dp'}{p'} \quad (6)$$

$$(d_e)_c^p=-(\lambda^*-\kappa^*)e_0\left(\frac{p'}{p_0'}\right)^{-(\lambda^*-\kappa^*)}\frac{dp'}{p'} \quad (7)$$

where e_0 and p_0' are the void ratio and the consolidation pressure at the initial state in the normal consolidation range, respectively.

(ii) As shown in Table 4, normally consolidated peat has a cohesion intercept c', but in order to simplify the equations, we let c' be equal to zero as in Fig. 19, and assume that the critical state lines become straight lines through the origin with the modified inclinations of M_c' or M_e' in the q vs. p' plane.

(iii) As noted in Fig. 20, from the results of loading-unloading tests under constant effective mean principal stress (p'=const.) on V and H specimens, as well as the assumption of Cambridge theory for clay soils, it can be assumed also in the case of peat that the only elastic component of strain that occurs during shear is the volumetric strain, and that there is never any elastic component of shear strain ; thus,

$$\left.\begin{aligned}(d_v)^e&=\frac{e_0}{1+e}\left[(\lambda^*-\kappa^*)\left(\frac{p'}{p_0'}\right)^{-(\lambda^*-\kappa^*)}-\lambda^*\left(\frac{p'}{p_0'}\right)^{-\lambda^*}\right]\frac{dp'}{p'}\\(d_v)_d^e&=0,\quad d\varepsilon_s^e=0\end{aligned}\right\} \quad (8)$$

where $(d_v)^e$ is the elastic component of the total volumetric strain increment, $(d_v)_d^s$ is the elastic component of the volumetric strain increment due to the deviatoric stress increment, and $d\varepsilon_s^e$ is the elastic component of the deviatoric strain increment.

(iv) For undrained shear, from Eqs. (4) and (5), the equivalent dilatancy $F(\eta)$, which is assumed to be a function of the stress ratio $\eta=q/p'$ (Mitachi et al (1979)), is represented as follows :

$$F(\eta)=-\frac{e_0}{1+e_0}\left[1-\left(\frac{p'}{p_0'}\right)^{-\lambda^*}\right] \quad (9)$$

where $F(\eta)$ is the volumetric strain due to the deviatoric stress component, which is calculated by subtracting the change of pore water pressure due to the increment of mean principal stress from the observed total change of pore water pressure during undrained shear.

Basic Stress-Strain Equations

Referring to existing theories and using the assumptions described in the preceding section, the basic equations of stress-strain relationships for isotropically normally consolidated peat can be derived. From Eqs. (4), (5) and (9), the change of total void ratio during shear is represented by the following equation :

$$d_e=-\lambda^* e_0\left(\frac{p'}{p_0'}\right)^{-\lambda^*}\frac{dp'}{p'}-(1+e_0)F'(\eta)d\eta \tag{10}$$

where $F'(\eta)$ is the differential form of $F(\eta)$. Accordingly, the equation of the state boundary surface is given by integrating Eq. (10) with the initial conditions $e=e_0$ and $p'=p_0'$ at $\eta=0$ as follows :

$$e=e_0\left(\frac{p'}{p_0'}\right)^{-\lambda^*}-(1+e_0)F(\eta) \tag{11}$$

Also, by integration of Eq. (6), the equation of the elastic wall is given as follows :

$$e-e_0=e_0\left[-\left(\frac{p'}{p_0'}\right)^{-(\lambda^*-\kappa^*)}+\left(\frac{p'}{p_0'}\right)^{-\lambda^*}\right] \tag{12}$$

By combining Eq. (12) with Eq. (11), the equation of the yield locus is expressed as follows :

$$e_0\left[\left(\frac{p'}{p_0'}\right)^{-(\lambda^*-\kappa^*)}-1\right]-(1+e_0)F(\eta)=0 \tag{13}$$

Assuming the normality condition to be applied, the basic equations of incremental stress-strain relationships are given as follows :

$$(d_v)^p=\frac{1+e_0}{1+e}\left[\frac{e_0(\lambda^*-\kappa^*)}{1+e_0}\left(\frac{p'}{p_0'}\right)^{-(\lambda^*-\kappa^*)}\frac{dp'}{p'}+F'(\eta)d\eta\right] \tag{14}$$

$$d\varepsilon_s^p=d\varepsilon_s=-\frac{1+e_0}{1+e}\left[\frac{e_0(\lambda^*-\kappa^*)}{1+e_0}\left(\frac{p'}{p_0'}\right)^{-(\lambda^*-\kappa^*)}\times\frac{dp'}{p'}+F'(\eta)d\eta\right]\times\left[\frac{F'(\eta)}{F'(\eta)\eta-\frac{e_0(\lambda^*-\kappa^*)}{1+e_0}\left(\frac{p'}{p_0'}\right)^{(*y-*\gamma)-}}\right] \tag{15}$$

$$d_v=\frac{1+e_0}{1+e}\left[\frac{\lambda^* e_0}{1+e_0}\left(\frac{p'}{p_0'}\right)^{-\lambda^*}\frac{dp'}{p'}+F'(\eta)d\eta\right] \tag{16}$$

where $(d_v)^p$ is the plastic component of the total volumetric strain increment d_v and $d\varepsilon_s^p$ is the plastic component of the deviatoric strain increment $d\varepsilon_s$. In the undrained shear test, applying the conditions $d_v=0$ and $e=e_0$, the equations of effective stress path, incremental stress-strain relationship and pore water pressure become as follows :

$$\left(\frac{p'}{p_0'}\right)=\left[1+\left(\frac{1+e_0}{e_0}\right)F(\eta)\right]^{-1/\lambda^*} \tag{17}$$

$$\frac{d\varepsilon_s}{d\eta}=\left[\left(\frac{\lambda^*-\kappa^*}{\lambda^*}\right)\left\{1+\left(\frac{1+e_0}{e_0}\right)F(\eta)\right\}^{-\kappa^*/\lambda^*}-1\right]\times\{F'(\eta)\}^2\Big\}\Big/\left[\eta F'(\eta)-\frac{e_0(\lambda^*-\kappa^*)}{1+e_0}\times\left\{1+\left(\frac{1+e_0}{e_0}\right)F(\eta)\right\}^{\left(\frac{\lambda^*-\kappa^*}{\lambda^*}\right)}\right] \tag{18}$$

$$\Delta u=p_0'\left[\left(\frac{\eta}{3}-1\right)\left\{\left(\frac{1+e_0}{e_0}\right)F(\eta)+1\right\}^{-1/\lambda^*}+1\right] \tag{19}$$

where Δu is the excess pore water pressure in the UCL and UEU Tests, with the total stress path represented by $q=3$ $(p-p_0')$. Accordingly, if the $F(\eta)$ vs. η relationship and the values of e_0, p_0', λ^* and κ^* are known, the calculation of undrained stress-strain relationships for normally consolidated peat will become possible.

Verification

In this section, the validity of the present method for predicting the stress-strain relationships of peat is examined by using the data from the triaxial tests under undrained compression and extension conditions mentioned previously. The undrained stress-strain equations shown as Eqs. (17)-(19) are based on the function of $F(\eta)$. Therefore, in order to predict accurately the stress-strain behavior, it is necessary to determine the appropriate function of $F(\eta)$. Then, based on the typical data in the UCL and UEU Tests on V and H specimens of peat with an ignition loss of about 70%, the values of $F(\eta)$ for any stress ratio calculated

from Eq. (10) are plotted against stress ratio η in Figs. 21(a)-(c). In these figures, the solid curves are $F(\eta)$ vs. η relationships which were calculated in order to represent appropriately the relationships which were observed. From these results, $F(\eta)$ for V and H specimens under compression and for H-specimens under extension can be approximated by the exponential and linear functions of η. That is, the $F(\eta)$ vs. η relationships for normally consolidated peat can be

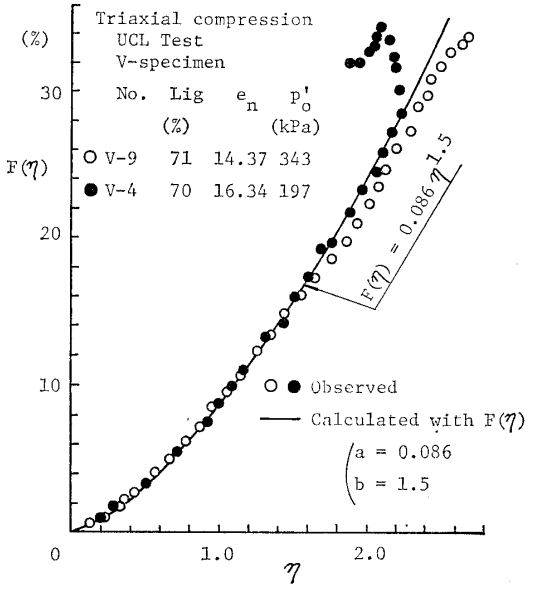

Fig. 21(a). $F(\eta)$ vs. η relationship for V-specimens in UCL Test

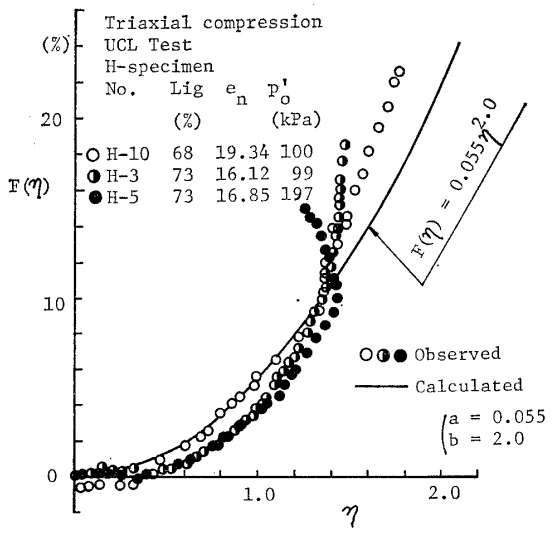

Fig. 21(b). $F(\eta)$ vs. η relationship for H-specimens in UCL Test

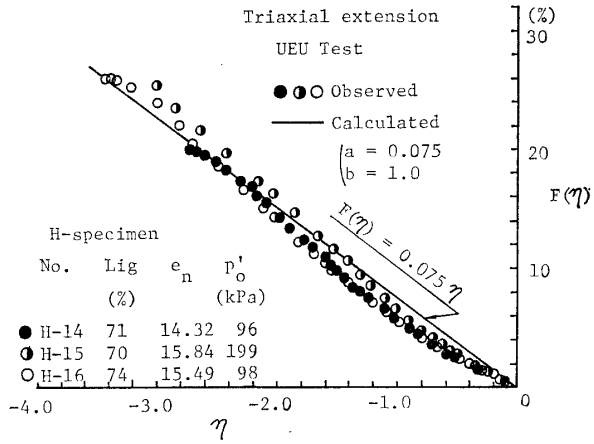

Fig. 21(c). $F(\eta)$ vs. η relationship for H-specimens in UEU Test

represented as follows :

$$F(\eta) = a\eta^b \qquad (20)$$

where a and b are experimental coefficients. Also, as can be seen in Fig. 22, from the results of the UCL Test on V-specimens of 10%-85%, the effect of the amount of organic matter in the range equivalent dilatancy behavior of peat will be approximately represented by the same exponential function of η with different values of the coefficient a. The degree of influence of the amount of or-

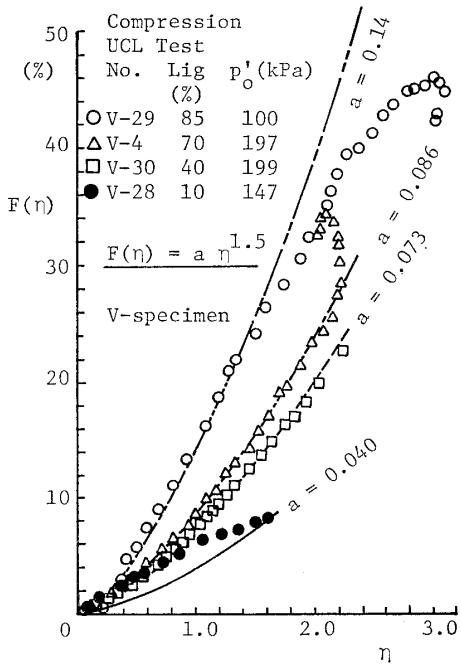

Fig. 22. Equivalent dilatancy behavior for V-specimens with different amounts of organic matter

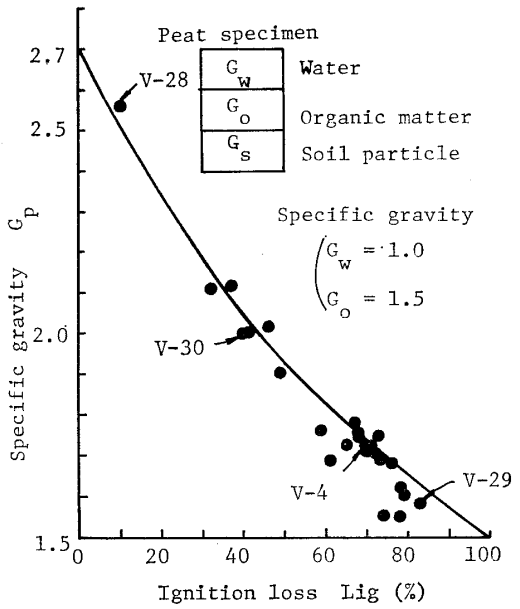

Fig. 23. Degree of amount of organic matter

ganic matter on individual specimens is shown as the positions plotted on the specific gravity G_p vs. ignition loss L_{ig} plane in Fig. 23. In this figure, the solid curve is represented by the following equation :

$$G_p=\frac{G_sG_0}{G_0(1-L_{ig}/100)+G_sL_{ig}/100} \quad (21)$$

where G_p is the specific gravity of the peat specimen, and G_w, G_s and G_0 represent specific gravity of water, of soil particles, and the organic matter itself, and these values are assumed as $G_w=1.0$, $G_s=2.7$ and $G_0=1.5$, respectively.

Then, substituting Eq. (20) into Eqs. (17)-(19), respectively, for the cases of the UCL and UEU Tests on V and H specimens, the comparisons of the experimental and calculated results of effective stress paths, axial strain vs. stress ratio and pore water pressure vs. axial strain relationships are shown in Figs. 24-26. The coefficients prepared for the calculations are indicated in Table 6. The values of λ^* can be determined from the isotropic consolidation process data prior to shear. By combining Eq. (18) with the conditions at the critical state, $d\eta/d\varepsilon_s=0$ and $d\varepsilon_s>>0$, the values of κ^* can be obtained from the following equation (Mitachi et al,

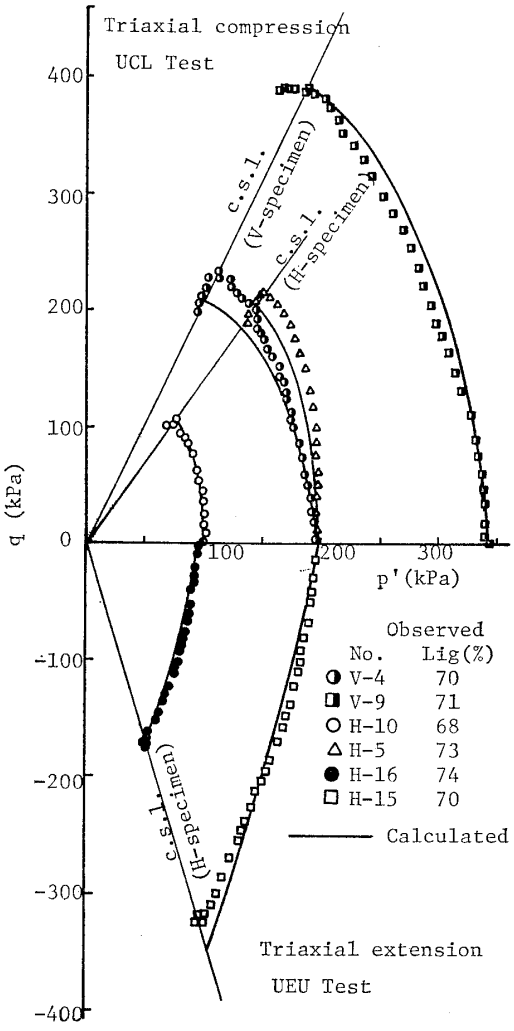

Fig. 24. Comparison of calculated effective stress paths with observed ones

1979 ; Yamaguchi et al, 1983) :

$$\kappa^*=\lambda^*+\frac{\lambda^*}{2F(M')}\left[\frac{e_0}{1+e_0}-\sqrt{\left(\frac{e_0}{1+e_0}\right)^2+\frac{4M'F'(M')F(M')}{\lambda^*}}\right] \quad (22)$$

where $F'(M')$ and $F(M')$ are $F'(\eta)$ and $F(\eta)$ at $\eta=M'$, respectively. The measured values of κ^* were very close to those obtained from Eq. (22). Also, the modified values of M' are dependent on the magnitude of the cohesion intercept c', but these values determined from the normally consolidated specimens in the range of consolidation pressures between 100 kPa and 350 kPa were about 0.98−1.1 times the measured values of M.

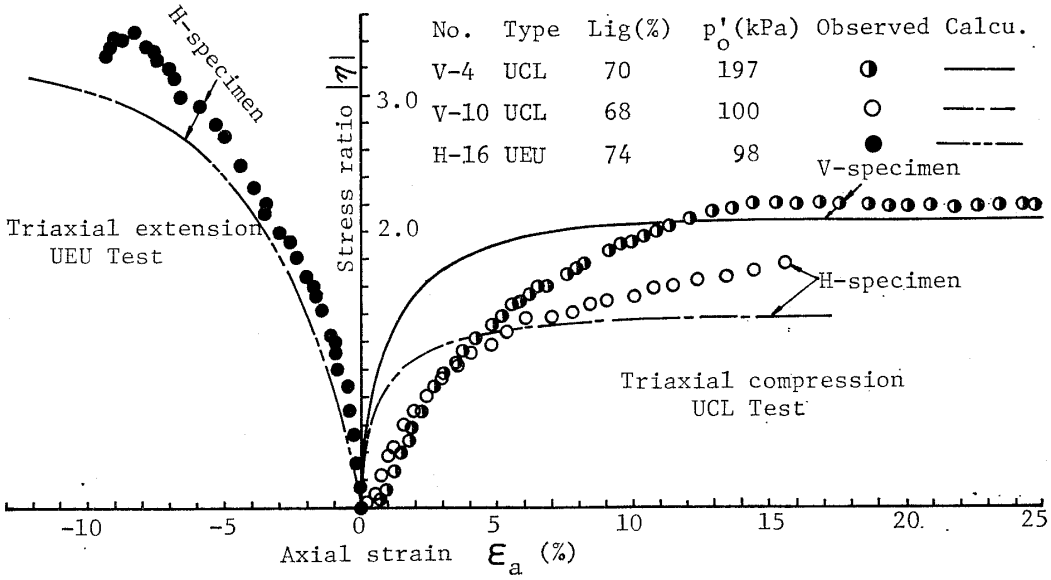

Fig. 25. Comparison of calculated stress ratio vs. axial strain relationships with observed ones

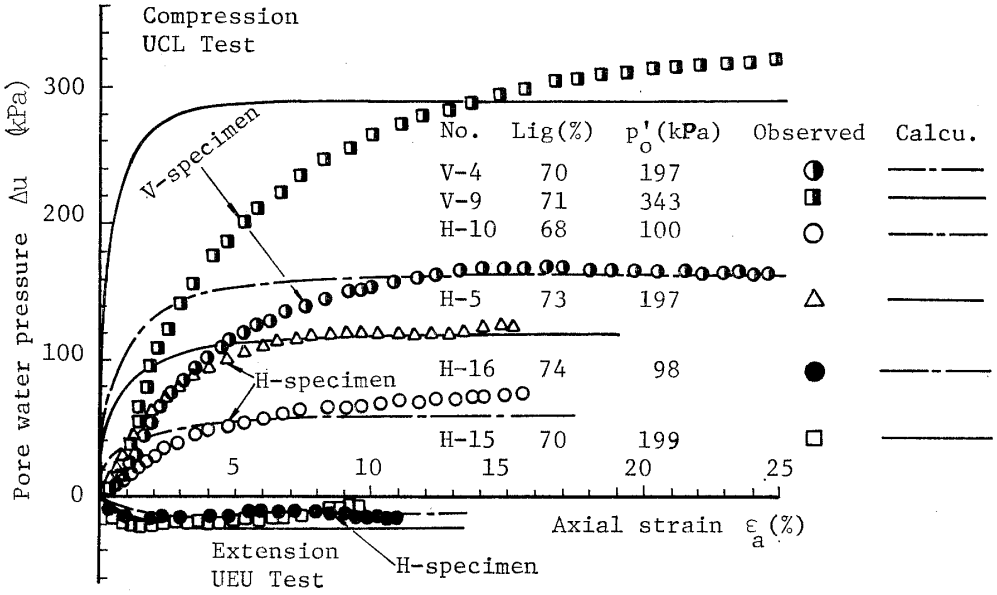

Fig. 26. Comparison of calculated pore water pressure vs. axial strain relationships with observed ones

As seen from Fig. 24, the calculated stress paths agree fairly well with the observed ones, because the stress paths predicted by Eq. (17) are based on the dilatancy functions which are experimentally derived from the observed $F(\eta)$ vs. η relationships. If the experimental relationships for dilatancy vs. stress ratio relationships are simulated closely by the dilatancy function, it will be natural that the calculated stress paths agree with the experimental results. On the other hand, it can be seen that the degree of agreement between the experimental and calculated values for stress ratio vs. axial strain and pore water pressure vs. axial strain curves is lower than that for the stress paths. In particular, for the results of the UCL Test on V-specimens it was found that the calculated values exceed the observed values of the strain increments for changes of η at

Table 6. Values of coefficients used for calculation of stress-strain relationships

No.	L_{ig}(%)	p_0'(kPa)	e_0	λ^*	a	b	M'	Tests
V-4	70	197	5.052	0.450	0.086	1.5	2.1	UCL
V-9	71	343	3.463	0.435	0.086	1.5	2.1	(V-specimen)
H-3	73	99	6.643	0.387	0.055	2.0	1.4	
H-5	73	197	4.975	0.394	0.055	2.0	1.4	UCL
H-10	68	100	6.684	0.428	0.055	2.0	1.4	(H-specimen)
H-14	71	96	6.284	0.388	0.075	1.0	3.3	
H-15	70	199	4.828	0.413	0.075	1.0	3.3	UEU
H-16	74	98	6.408	0.401	0.075	1.0	3.3	(V-specimen)
V-28	10	147	1.605	0.170	0.040	1.5	—	
V-29	85	100	6.470	0.432	0.140	1.5	—	UCL
V-30	40	199	3.147	0.375	0.073	1.5	—	(V-specimen)

small values of η. However, as a first approximation, the present method——which was derived from the existing theories on the stress-strain relationships for normally consolidated clay soils——would be very useful in reaching a systematic understanding of the undrained shear behavior of normally consolidated fibrous peat.

CONCLUSIONS

1) As well as in the case of inorganic soils, the shear behavior of fibrous peat under undrained compression or extension conditions is not affected by the magnitude of confining pressure prior to shear or by the loading path during shear, and can be discussed in terms of the effective stress.

2) The aniostropic fabric of fibrous peat still remains after the end of isotropic consolidation and, to a considerable extent, anisotropic shear behavior is observed.

3) The undrained shear behavior of peat under compression conditions is quite distinct from that under extension conditions due to the effect of vegetal fibers ; however, the behavior under both compression and extension conditions can be normalized by the consolidation pressure.

4) Normally consolidated fibrous peat has a cohesion intercept and shows very large values in undrained strength parameters compared with those of inorganic soils. These values are closely related to the amount of organic matter involved.

5) As a first approximation, the proposed method by the present authors, which was derived from the existing theories on the stress-strain relationships for clay soils by reflecting the effect of fabric anisotropy in the equivalent dilatancy vs. stress ratio relationships, would be very useful in arriving at a quantitative understanding of the shear behavior of normally consolidated specimens of fibrous peat under compression and extension conditions.

NOTATION

A_f=pore pressure coefficient at failure

$F(\eta)$, $F'(\eta)$=dilatancy function and differential form of $F(\eta)$

L_{ig}=ignition loss

G_0, G_p, G_s, G_w=specific gravities of the organic matter itself, peat, soil particles and water

c'=effective cohesion intercept

v=volumetric strain

e_0, p_0'=e and p' at the end of consolidation

m=vertical intercept in the q_f vs. p_f' plane

p', q=effective mean principal stress and deviator stress, $p'=(\sigma_a'+2\sigma_r')/3$ and $q=\sigma_a-\sigma_r$

p_f', q_f=p' and q at failure

M, M'=inclination of critical state line in the q_f vs. p_f' plane

d_e, $(d_e)_c$, $(d_e)_d$=increment of void ratio, components due to effective mean principal stress increment and deviatoric stress increment of d_e

$(d_e)_c^e$, $(d_e)_c^p$=elastic and plastic components of $(d_e)_c$

$(d_e)_d^e$, $(d_e)_d^p$=elastic and plastic components of

$(d_e)_d$

d_v, $(d_v)_c$, $(d_v)_d$ = increment of volumetric strain, components due to effective mean principal stress increment and deviatoric stress increment of d_v

$(d_v)^e$, $(d_v)^p$ = elastic and plastic components of d_v

$d\varepsilon_s$, $d\varepsilon_s^e$, $d\varepsilon_s^p$ = increment of deviatoric strain, elastic and plastic components of $d\varepsilon_s$, $d\varepsilon_s = d\varepsilon_a - d_v/3$

Δu = excess pore water pressure

η = shear stress ratio, $\eta = q/p'$

ε_a, ε_f = axial strain and ε_a at failure

λ^* = inclination of normal consolidation line in the ln e vs. ln p' plane

κ^* = inclination of swelling line in the ln e vs. ln p' plane or value calculated from Eq. (22)

σ_c' = consolidation pressure

σ_a, σ_a' = total and effective axial stresses

σ_r, σ_r' = total and effective radial stresses

σ_{af}', σ_{rf}' = σ_a' and σ_r' at failure

REFERENCES

1) Adams, J. I. (1962) : "Laboratory compression test on peat," Ontario Hydro Research News, Third quarter, pp. 35-40.

2) Adams, J. I. (1965) : "The engineering behaviour of a Canadian Muskeg," Proc. of 6 th ICSMFE, Vol. 1, pp. 3-7.

3) Edil, T. B. and Dhowian, A. W. (1981) : "At-rest lateral pressure of peat soils," Proc., ASCE, Vol. 107, No. GT 2, pp. 201-217.

4) Hanrahan, E. T. (1954) : "An investigation of some physical properties of peat," Géotech., Vol. 4, No. 3, pp. 108-123.

5) Mitachi, T. and Kitago, S. (1979) : "The influence of stress history and stress system on the stress-strain-strength properties of saturated clay," Soils and Foundations, Vol. 19, No. 2, pp. 45-61.

6) Oikawa, H. and Miyakawa, I. (1980) : "Undrained shear characteristics of peat," Jour. of JSSMFE, Vol. 20, No. 3, pp. 92-100 (in Japanese).

7) Ozden, Z. S. and Wilson, N. E. (1970) : "Shear strength characteristics and structure of organic soils," Proc. of 13 th Muskeg Research Conf. NRC, Canada, pp. 8-26.

8) Roscoe, K. H., Schofield, A. N. and Thurairajah, A. (1963) : "Yielding of clays in states wetter than critical," Géotech., Vol. 13, No. 3, pp. 211-240.

9) Tsushima, M., Miyakawa, I. and Iwasaki, T. (1977) : "Some investigations on shear strength of organic soil," Tsuchi-to-Kiso, JSSMFE, No. 235, pp. 13-18 (in Japanese).

10) Tsushima, M. and Oikawa, H. (1982) : "Shear strength and dilatancy of peat," Jour. of JSSMFE, Vol. 22, No. 2, pp. 133-141 (in Japanese).

11) Yamaguchi, H., Mitachi, T. and Kitago, S. (1983) : "Prediction of stress-strain behavior of a clay taking effect of secondary consolidation into consideration," Jour. of JSSMFE, Vol. 23, No. 2, pp. 179-188 (in Japanese).